An improved embedded finite element formulation for investigating fluid flow behavior in fractured porous media

Danilo B. Cavalcanti[1,2], Cristian Mejia[3], Deane Roehl[1,3], Luiz F. Martha[1,3], Ignasi de Pouplana[2,4], Guillermo Casas[2]

[1] *Dept. of Civil and Environmental Engineering, Pontifical Catholic University of Rio de Janeiro*
Rua Marques de São Vicente 225, 22451-900 Gávea, Rio de Janeiro - RJ, Brazil
danilocavalcanti@aluno.puc-rio.br,
[2] *CIMNE - Centre Internacional de Metodes Numerics em Enginyeria*
Gran Capitán s/n, CIMNE, Edificio C1, Campus Nord, UPC, Gran Capitán s/n, 08034 Barcelona, Spain
gcasas@cimne.upc.edu mailto:somebody3@somewhere.edu
[3] *Tecgraf Institute, Pontifical Catholic University of Rio de Janeiro*
22451-000, RJ, Brazil
crisms@tecgraf.puc-rio.br; deane@tecgraf.puc-rio.br; lfm@tecgraf.puc-rio.br
[4] *Departament d'Enginyeria Civil i Ambiental (DECA), Universitat Politècnica de Catalunya (UPC)*
Campus Nord, C. Jordi Girona, 1-3, 08034 Barcelona, Spain
ignasi.de.pouplana@upc.edu

Abstract. Discontinuities, such as fractures and geological faults, are present in several geological models where a fluid flow analysis is performed. In cases where the discontinuity filling material has a lower permeability than the matrix, this discontinuity will act as a barrier to fluid flow in the porous media. On the other hand, fluid flow is enhanced in the absence of filling material or in the highly porous case. Embedded formulations have become attractive to model discontinuities over the last decades since they do not require mesh conformity. However, the literature lacks a formulation fully developed in the context of the Finite Element Method capable of modeling discontinuities that act like barriers to fluid flow in transient problems. This paper presents an improved embedded finite element formulation to investigate fluid flow behavior in fractured porous media. The proposed approach includes additional degrees-of-freedom representing the pressure drop between fracture surfaces and the fluid pressure within the fracture. Single-phase flow is considered. Darcy's law governs fluid flow through the porous media, while the cubic law of parallel plates controls the fluid flow inside the fracture channel. A numerical example comparing the results with a model with interface elements modeling the discontinuity is compared to the embedded formulation. The numerical results demonstrate the capability and limitations of the proposed approach to capture the influence of discontinuities on fluid flow behavior in porous media.

Keywords: Embedded finite element, fluid flow in porous media, barriers.

1 Introduction

The fluid flow in a geological model with the presence of discontinuities, such as fractures and geological faults, is highly dependent on the discontinuities' hydraulic properties. If the discontinuity filling material is less permeable than the matrix, it will act as a barrier to fluid flow in the porous media. On the other hand, fluid flow is enhanced in the absence of filling material or in the highly porous case.

In the context of the Finite Element Method, different approaches to model this problem can be found in the literature. Here we highlight the discrete modeling approach, using interface elements, and embedded formulations, which in general, involve applying an enrichment to the discretized field. This last approach has become attractive over the last decades since it does not require mesh conformity.

The embedded formulation in this study is based on the Strong Discontinuity Approach (SDA), with the enrichment degrees of freedom associated with the discontinuity. In the literature, Callari and Armero [1], Alfaiate et al. [2], and Benkemoun et al. [3] used the embedded formulations based on the SDA to model fluid-flow problems in porous media. Still these studies, the transversal flow in the discontinuity was not considered. Recently, Damirchi et al.. [4] presented an embedded finite element formulation capable of modeling both longitudinal and transversal flow in the discontinuity, achieving a finite element with similar behavior to double-node interface elements in steady-state single-phase fluid flow problems.

In this paper, the formulation presented by Damirchi et al. [4] is extended to transient problems. The behavior of the finite element is then evaluated by comparing it with a model using an interface element.

2 Governing equations

Consider the problem presented in Figure 1 with a domain Ω closed by a boundary Γ and composed by the union of the boundary Γ_p and Γ_q, associated with the essential and natural boundary conditions, respectively. The A discontinuity, Γ_d, crosses the domain and separates it into two sub-domains, Ω^+ and Ω^-. Their definition is based on the normal vector to the discontinuity surface, $\mathbf{n}_d$, such that Ω^+ is the sub-region at which the normal vector $\mathbf{n}_d$ points.

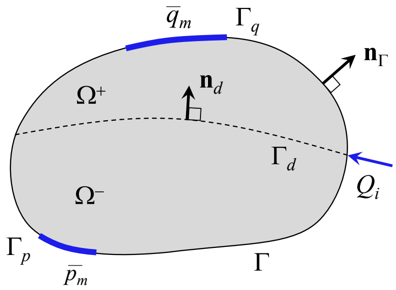

Figure 1. Problem domain and boundary conditions

Two continuity equations govern the fluid flow problem in a fractured porous media. Neglecting the deformability of the solid skeleton and using Darcy's law, the continuity equation that defines fluid flow through the porous media can be written as:

$$\left(\frac{\alpha-\phi}{K_s}+\frac{\phi}{K_f}\right)\frac{\partial p_m}{\partial t}-\nabla\cdot\left(\frac{\mathbf{k}}{\mu}\nabla p_m\right)=0,\ \mathbf{x}\in\Omega\setminus\Gamma_d \tag{1}$$

where p_m is the pressure field in the porous media, $\mathbf{k}$ is the permeability tensor, μ_f is the dynamic viscosity of the fluid, α is Biot's coefficient, ϕ is the porosity, K_s is the bulk modulus of the solid, and K_f is the bulk modulus of the fluid.

The second governing equation is the continuity equation of the fluid flow inside the discontinuity:

$$\frac{\partial q_f}{\partial s}+q_T+q_B=0,\ \mathbf{x}\in\Gamma_d \tag{2}$$

where q_f is the longitudinal mass flow, q_T, and q_B are the transversal mass flows through the top and bottom boundaries of the discontinuity, respectively, and s is the longitudinal coordinate along the discontinuity. These flows are described in terms of the pressure field along the top, p_T, middle, p_f, and bottom, p_B, planes of the discontinuity:

$$q_T=c_T\left(p_f-p_T\right) \tag{3}$$

$$q_B=c_B\left(p_f-p_B\right) \tag{4}$$

$$q_f=-\frac{w^3}{12\mu_f}\frac{\partial p_f}{\partial s} \tag{5}$$

where c_T and c_B are the leak-off parameters, and w is the discontinuity normal aperture.

3 Discretization of the governing equations

Initially, the problem is discretized following the same strategy as XFEM [5]. Two sets of degrees of freedom are defined per node to describe the pressure field: **p** and **a**. The first set is associated with the regularized pressure field, and the second set is associated with the enriched pressure field. For example, Figure 2 illustrates a linear quadrilateral finite element with an embedded discontinuity.

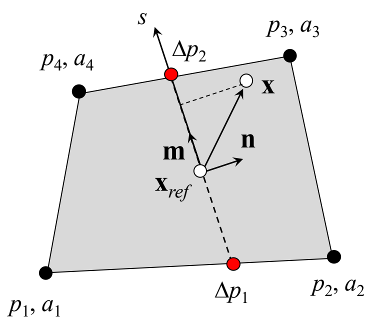

Figure 2. Quadrilateral finite element with an embedded discontinuity

The pressure field in the porous media is discretized as:

$$p_m(\mathbf{x},t) = \mathbf{N}(\mathbf{x})\left[\mathbf{p}(t) + \left(\mathcal{H}_{\Gamma_d}(\mathbf{x})\mathbf{I} - \mathbf{H}_d\right)\mathbf{a}(t)\right] \tag{6}$$

where matrix **N** is the usual shape function matrix of the finite element, $\mathcal{H}_{\Gamma d}$ is the Heaviside function, which assumes one if the point is inside the sub-domain Ω^+ and zero if the point is inside the sub-domain Ω^-, and $\mathbf{H}_d$ is a diagonal matrix with the Heaviside function evaluated at the element nodes.

The longitudinal pressure in the discontinuity mid-plane is taken as an independent field, and is discretized as:

$$p_f(s,t) = \mathbf{N}_d(s)\,\mathbf{p}_f(t) \tag{7}$$

where $\mathbf{N}_d$ is a vector composed of one-dimensional Lagrange shape functions, and $\mathbf{p}_f$ is the vector with the pressure degrees of freedom in the discontinuity mid-plane.

3.1 Discretized weak form

The weak form of the governing equations (1) and (2) is obtained by applying the Galerkin method followed by the Divergence theorem. Then, substituting the discretization of the pressure fields defined in equations (6) and (7), the following system is obtained:

$$\begin{bmatrix} \mathbf{S}_m & \mathbf{0} \\ \mathbf{0} & \mathbf{0} \end{bmatrix} \dot{\mathbf{P}}(t) + \begin{bmatrix} \mathbf{H}_m + \mathbf{L}_{1,t} + \mathbf{L}_{1,b} & -\mathbf{L}_2 \\ -\mathbf{L}_2^T & \mathbf{L}_3 + \mathbf{H}_f \end{bmatrix} \mathbf{P}(t) = \begin{Bmatrix} \mathbf{q} \\ \mathbf{q}_f \end{Bmatrix} \tag{8}$$

where:

$$\mathbf{P} = \begin{bmatrix} \mathbf{p}^T & \mathbf{a}^T & \mathbf{p}_f^{\,T} \end{bmatrix}^T \tag{9}$$

$$\mathbf{S}_m = \int_{\Omega \setminus \Gamma_d} \begin{bmatrix} \mathbf{N}(\mathbf{x}) & \mathbf{N}(\mathbf{x})\left(\mathcal{H}_{\Gamma_d}(\mathbf{x})\mathbf{I} - \mathbf{H}_d\right) \end{bmatrix}^T \frac{1}{M} \begin{bmatrix} \mathbf{N}(\mathbf{x}) & \mathbf{N}(\mathbf{x})\left(\mathcal{H}_{\Gamma_d}(\mathbf{x})\mathbf{I} - \mathbf{H}_d\right) \end{bmatrix} d\Omega \tag{10}$$

$$\mathbf{H}_m = \int_{\Omega \setminus \Gamma_d} \left[\nabla \mathbf{N}(\mathbf{x}) \quad \nabla \mathbf{N}(\mathbf{x}) \left(\mathcal{H}_{\Gamma_d}(\mathbf{x}) \mathbf{I} - \mathbf{H}_d \right) \right]^T \frac{1}{\mu_f} \begin{bmatrix} \mathbf{k} & \mathbf{0} \\ \mathbf{0} & \mathbf{k} \end{bmatrix} \left[\nabla \mathbf{N}(\mathbf{x}) \quad \nabla \mathbf{N}(\mathbf{x}) \left(\mathcal{H}_{\Gamma_d}(\mathbf{x}) \mathbf{I} - \mathbf{H}_d \right) \right] d\Omega \tag{11}$$

$$\mathbf{L}_2 = \int_{\Omega \setminus \Gamma_d} \left[\mathbf{N}(\mathbf{x}) \quad \mathbf{N}(\mathbf{x}) (\mathbf{I} - \mathbf{H}_d) \right]^T c_T \; \mathbf{N}_d(\mathbf{x}) d\Omega + \int_{\Omega \setminus \Gamma_d} \left[\mathbf{N}(\mathbf{x}) \quad -\mathbf{N}(\mathbf{x}) \mathbf{H}_d \right]^T c_B \; \mathbf{N}_d(\mathbf{x}) d\Omega \tag{12}$$

$$\mathbf{L}_{1,t} = \int_{\Omega \setminus \Gamma_d} \left[\mathbf{N}(\mathbf{x}) \quad \mathbf{N}(\mathbf{x}) (\mathbf{I} - \mathbf{H}_d) \right]^T c_T \left[\mathbf{N}(\mathbf{x}) \quad \mathbf{N}(\mathbf{x}) (\mathbf{I} - \mathbf{H}_d) \right] d\Omega \tag{13}$$

$$\mathbf{L}_{1,b} = \int_{\Omega \setminus \Gamma_d} \left[\mathbf{N}(\mathbf{x}) \quad -\mathbf{N}(\mathbf{x}) \mathbf{H}_d \right]^T c_B \left[\mathbf{N}(\mathbf{x}) \quad -\mathbf{N}(\mathbf{x}) \mathbf{H}_d \right] d\Omega \tag{14}$$

$$\mathbf{L}_3 = \int_{\Gamma_d} (c_T + c_B) \mathbf{N}_d^T(\mathbf{x}) \mathbf{N}_d(\mathbf{x}) d\Gamma \tag{15}$$

$$\mathbf{H}_f = \int_{\Gamma_d} \frac{\partial \mathbf{N}_d^T(\mathbf{x})}{\partial s} \frac{w^3}{12 \mu_f} \frac{\partial \mathbf{N}_d(\mathbf{x})}{\partial s} d\Gamma \tag{16}$$

3.2 Proposed embedded formulation

This embedded finite element formulation aims to reduce the number of enrichment degrees of freedom. Then, instead of describing the discontinuity in the pressure field using additional degrees of freedom at the nodes of the finite element, as done in XFEM, it uses the jump in the pressure field evaluated along the embedded discontinuity, as shown in Figure 2. To achieve this, the following transformation must be defined:

$$\mathbf{a}(t) = \mathbf{T} \Delta \mathbf{p}(t) \tag{17}$$

If a constant jump in the pressure field is assumed along the longitudinal coordinate s, then the matrix $\mathbf{T}$ is simply:

$$\mathbf{T} = [1 \quad 1 \quad 1 \quad 1]^T \tag{18}$$

If a linear jump in the pressure field is assumed along the longitudinal coordinate s:

$$\Delta p_m(s,t) = \frac{\Delta p_1 + \Delta p_2}{2} + s \, \frac{\Delta p_2 - \Delta p_1}{l_d} \tag{19}$$

where l_d is the discontinuity length inside the element, and Δp_1 and Δp_2 are the jumps in the pressure field at the nodes where the discontinuity intersects the element.

By assuming that the transmission of the jump in the pressure field that happens in the discontinuity to the continuum occurs completely in the normal direction:

$$\mathbf{T} = \left[\mathbf{T}_i^T(\mathbf{x}_1) \quad \mathbf{T}_i^T(\mathbf{x}_2) \quad \mathbf{T}_i^T(\mathbf{x}_3) \quad \mathbf{T}_i^T(\mathbf{x}_4) \right]^T \tag{20}$$

with:

$$\mathbf{T}_i(\mathbf{x}) = \left[\frac{1}{2} - \frac{\mathbf{m} \cdot (\mathbf{x} - \mathbf{x}_{ref})}{l_d} \quad \frac{1}{2} + \frac{\mathbf{m} \cdot (\mathbf{x} - \mathbf{x}_{ref})}{l_d} \right] \tag{21}$$

This later definition is the same one presented by Damirchi et al. [4]. They discuss that this definition of this transmission matrix, **T**, promotes a rigid-body transfer of the pressure jumps along the interface to the continuum. The consequence of this is that the product **B T** leads to a zero matrix. In steady-state problems, this simplifies the implementation calculations since the parts in the fluid flow matrix that are multiplied by the Heaviside function, shown in equation (11), go to zero. Then, there is no need to perform a subdivision of the element domain to do the numerical integration of the element matrices.

Since this paper analyzes a transient problem, and the compressibility matrices are present, equation 10, then a subdivision of the element domain is required to perform the numerical integration.

4 Solution scheme

A fully implicit time integration scheme was adopted.

$$\mathbf{P}(t_{n+1}) = \mathbf{P}(t_n) + \Delta t\, \dot{\mathbf{P}}(t_{n+1}) \tag{22}$$

where t_{n+1} corresponds to the current time, t_n to the previous one, and Δt is the time step.

By substituting in (8), the system of equations presented in equation (23) is obtained.

$$(\mathbf{S} + \Delta t\, \mathbf{H})\mathbf{P}(t_{n+1}) = \Delta t\, \mathbf{Q} + \mathbf{S}\,\mathbf{P}(t_n) \tag{23}$$

5 Numerical example

For all numerical examples, the following properties were adopted: the hydraulic conductivity of 1.1574e-5 m/s, the fluid dynamic viscosity of 1.0e-3 Pa s, the specific water weight of 9.81 kN/m³, and the discontinuity normal aperture is zero.

To validate the results obtained with the embedded formulation presented in this paper, the same problems were modeled with triple-node interface elements using the in-house code GeMA [6].

The problem analyzed consists of a square domain of 2 x 2 m, discretized with a single finite element using the embedded and discretized using two continuum elements and one interface element using discrete fracture model. A zero-pressure boundary condition is defined at the top edge of the domain and a discharge at the bottom edge. Two discharge conditions are considered: uniform and non-uniform.

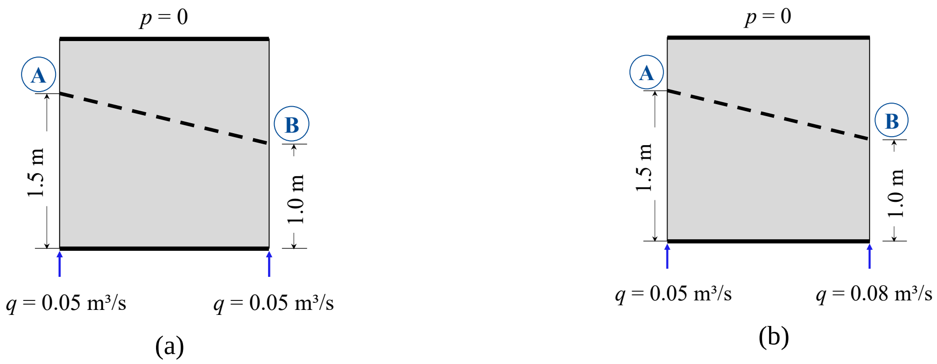

Figure 3. Geometry and boundary conditions of the example: (a) uniform discharge; (b) non-uniform discharge

5.1 Permanent analysis

The first example evaluates the capability of the proposed embedded formulation to model the presence of barriers inside the porous media. To do this, leak-off values equal to 1.0 m/(kPa s) and 1.0e-9 m/(kPa s) were assumed. The results for the uniform discharge case are shown in Figure 4.

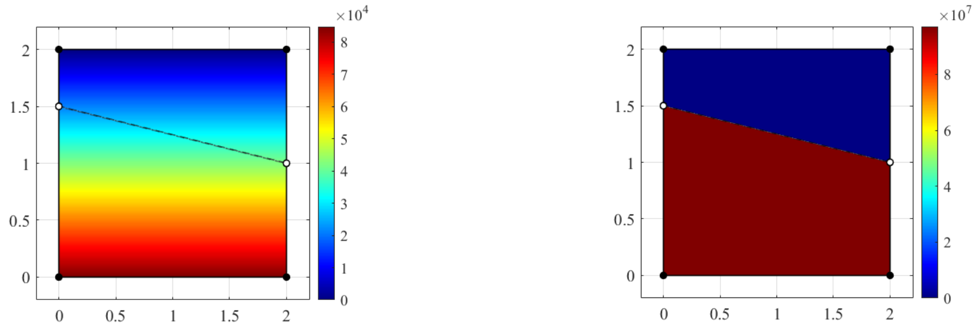

(a) (b)

Figure 4. Permanent analysis in the uniform discharge case. (a) $c_T = c_B$ = 1e-1 m/(kPa s); (b) $c_T = c_B$ = 1e-9 m/(kPa s)

In the uniform discharge case, the relative error between the embedded formulation and the interface element model of the pressure at the bottom nodes and the pressure jumps is of magnitude lower the 1e-12.

To analyze the non-uniform discharge case, the pressure field along the left edge was evaluated for the same two leak-off parameters, as shown in Figure 5.

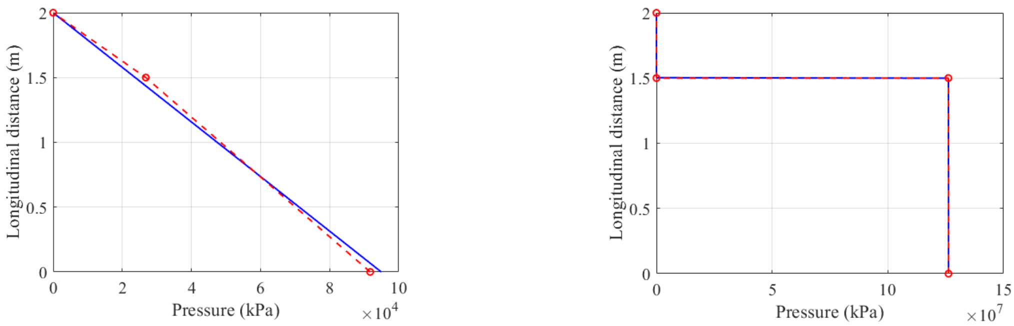

(a) (b)

Figure 5. Permanent analysis in the non-uniform discharge case. (a) $c_T = c_B$ = 1e-1 m/(kPa s); (b) $c_T = c_B$ = 1e-9 m/(kPa s)

In the non-uniform discharge case, there is a difference in the values obtained with the two models, as can be seen in Figure 5. This difference is justified by the fact that the model using an interface element can capture the change in the pressure gradient due to the presence of the discontinuity, and this is not taken into account in the embedded finite element formulation presented in this paper. An improvement in the matrix **T**, equation (17), would be required to achieve this.

5.2 Transient analysis

To perform a transient analysis, a compressible porous media was considered with the bulk modulus of the solid equal to 1.0e9 kPa, and the bulk modulus of the fluid equal to 2.0e6 kPa. Only the case of a uniform discharge is analyzed. The time increment was kept constant for the transient analysis and equal to 0.1 s, and the final analysis time was set as 10.0 s.

Table 1 presents the results for the nodal pressures at the final time.

Table 1. Transient analysis: comparison with interface elements in the uniform discharge case with leak-off equal to 1e-9 m/(kPa s)

Value (kPa)	Interface element	Embedded	Relative error
Node pressure 1	2.63708867e6	2.6341902028e6	1.099E-03
Node pressure 2	2.64148780e6	2.6364200418e6	1.919E-03
Jump A	-2.60347152e6	-2.5965295736e6	2.666E-03
Jump B	-2.618313.38e6	-2.6172937932e6	3.894E-04

Despite the embedded formulation results still being close to those of the interface element model, the relative error increased from the magnitude of 1e-12 to 1e-3. This increase in the difference, even in the case of a uniform discharge, is justified as in the example of the permanent case in a non-uniform discharge. Now, a change in the pressure gradient is present in the results with interface elements, and this embedded formulation cannot capture this behavior.

6 Conclusions

This paper presented a study with embedded finite elements for fluid flow in porous media capable of modeling transversal flow through discontinuities. The embedded formulation is achieved through a transformation of the enrichment degrees of freedom based on the XFEM. The numerical example shows the capability of the formulation to control the transversal flow using the leak-off parameter and also a comparison of the present embedded formulation with a model using interface elements. The comparison was made for a permanent and a transient problem with different boundary conditions, which allowed us to see the difference in the two approaches due to the simplifications involved in the embedded formulation.

A simple example was presented, and allowed a better understanding of the present formulation. Therefore, the ongoing studies focus on applying the formulation to larger problems and extending it to a two-phase flow formulation.

Acknowledgments. The authors acknowledge the financial support from CAPES (in Portuguese, "Coordenação de Aperfeiçoamento de Pessoal de Nível Superior"). We are also thankful for the grant TED2021-130510A-I00 funded by MCIN/AEI/ 10.13039/501100011033 and by the “European Union NextGenerationEU/PRTR”.

Authorship statement. The authors hereby confirm that they are the sole liable persons responsible for the authorship of this work, and that all material that has been herein included as part of the present paper is either the property (and authorship) of the authors, or has the permission of the owners to be included here.

References

[1] C. Callari and F. Armero. “Finite element methods for the analysis of strong discontinuities in coupled poro-plastic media”. *Computer Methods in Applied Mechanics and Engineering*, vol. 191, pp. 4371-4400, 2002.
[2] J. Alfaiate, P. Moonen, L. J. Sluys and J. Carmeliet, J. “On the use of the strong discontinuity formulation for the modeling of preferential moisture uptake in fractured porous media”. *Computer Methods in Applied Mechanics and Engineering*, vol. 199, pp. 2828-2839, 2010.
[3] N. Benkemoun, R. Gelet, E. Roubin and J. B. Colliat. “Poroelastic two-phase material modeling: theorical formulation and embedded finite element method implementation”. *International Journal for Numerical and Analytical Methods in Geomechanics*. vol. 39, pp. 1255-1275, 2015.
[4] B. V. Damirchi, M. R. Carvalho, L. A. G. Bittencourt Jr., O. L. Manzoli and D. Dias-da-Costa. “Transverse and longitudinal fluid flow modelling in fractured porous media with non-matching meshes. *International Journal for Numerical and Analytical Methods in Geomechanics*. vol. 45, pp. 83-107, 2021.
[5] A. M. Khoei. Extended Finite Element Method: theory and applications. John Wiley & Sons, 2015.
[6] C. A. T. Mendes, M. Gattass, D. Roehl. “The gema framework - An innovative framework for the development of multiphysics and multiscale simulations”, in: *ECCOMAS Congr 2016 - Proc 7th Eur Congr Comput Methods Appl Sci Eng*, vol. 4, pp. 7886–7894, 2016.